Low-temperature anharmonic lattice deformations near rotator impurities: A quantum Monte Carlo approach

M. H. Müser, W. Helbing, P. Nielaba, and K. Binder
Institut für Physik, Johannes Gutenberg-Universität, KoMa 331, D-55099 Mainz, Federal Republic of Germany
(Received 11 October 1993)

At zero temperature the equilibrium structures of a system consisting of a quantum rotator (N_2) embedded in a relaxing lattice (Ar) surrounding are studied with a variational approach. With symmetric wave functions (*para*-N_2), we obtain a cubic lattice deformation near the rotator, while with antisymmetric wave functions (*ortho*-N_2), we obtain a tetragonal lattice deformation forming a stable oriented ground state. At low temperatures, we investigate the properties of this system with a quantum Monte Carlo simulation. On top of the tetragonal deformation the width of the nearest-neighbor oscillations follows classical "scaling" laws according to a harmonic approximation, while the static deformation turns out to be anharmonic. The Monte Carlo relaxation of the rotational degree of freedom occurs according to an Arrhenius law with an activation energy much lower than the local energy barriers.

PACS number(s): 61.20.Ja, 02.70.Lq, 05.30.−d, 61.72.−y

I. INTRODUCTION

Measurements of static properties of orientational glasses like $(N_2)_x(Ar)_{1-x}$ often show anomalous low temperature behavior, e.g., a specific heat proportional to the temperature, for reviews see Ref. [1]. In a similar system $(KCN)_x(KCl)_{1-x}$, one observes abnormal scattering behavior (triangle Bragg peaks) [2]. Such results can neither be explained by analytical theories where the coupling between rotational and translational degrees of freedom is treated on a mean-field-like level [3] nor by Edwards-Anderson-type models of orientational glasses [4], which omit the translational degree of freedom altogether. These anomalies may be attributed to the fact that the rotational degrees of freedom of the molecules freeze in and thus form local disordered arrangements of the orientation. The centers of mass of the particles are assumed to remain on a distorted ordered crystal lattice. Thus every rotator moves in a different local arrangement, which leads to a very individual distribution of the rotational eigenenergies eventually resulting in a linear specific heat, $C_p \propto T$. This temperature dependency is often [5] attributed to two-level systems, which also shows up in anomalous dynamical properties [6]. For a detailed understanding of such properties, computer simulations of realistic models would be rather desirable. A molecular dynamics study of a model for N_2-Ar mixtures has provided a rather satisfactory overall agreement of the simulated phase diagram [7] with experiment [8], but since in these works a *purely classical* approach was followed, the low-temperature properties of these systems cannot be addressed.

Here we investigate the properties of one rotator (N_2) with quantum rotational degrees of freedom, surrounded by a fcc lattice of classical (Ar) particles, we are thus studying the properties of $(N_2)_x(Ar)_{1-x}$ in the dilute limit, $x \to 0$. In Sec. II we define the Hamiltonian of our system and we describe the method, how we compute the statistical weight of one configuration at a given temperature. Further, in Sec. III we determine the ground state for *ortho*-N_2 and *para*-N_2 by a random walk of the translational degrees of freedom, after having computed the ground state and the first excited state within only cubic lattice deformations. The results of a quantum Monte Carlo treatment of the system at finite temperatures are presented in Sec. IV. In Sec. V we give an outlook and summary.

II. THE METHOD

One of the reasons of our investigation was the interest in the contribution of the lattice deformations, due to the presence of a (N_2) molecule, on the level splitting of the rotator. In a disordered medium these deformations are different for every rotator. Thus they induce a distribution of rotational eigenenergies and this in turn may lead to an abnormal low-temperature specific heat.

In order to be able to compute the statistical weight of one configuration and thus to apply the Metropolis procedure, we first define the Hamiltonian for the whole system.

$$\hat{\mathcal{H}} = T_{\mathrm{Ar}}(\{\mathbf{p}\}) + T_{\mathrm{N_2}}^{(\mathrm{trans})}(\mathbf{P}) + V_{\mathrm{Ar-Ar}}(\{\mathbf{r}\}) + \hat{\mathcal{H}}_{\mathrm{rot}}(\{\mathbf{r}\}, \mathbf{R}_0, \vartheta, \varphi), \tag{1}$$

with the kinetic translational energies $T_{\mathrm{Ar}}, T_{\mathrm{N_2}}^{(\mathrm{trans})}$ for the Ar and N_2 particles, the Lennard-Jones (6-12) interaction energy [7] $V_{\mathrm{Ar-Ar}}$ for the Ar particles, and

$$\hat{\mathcal{H}}_{\mathrm{rot}} = \frac{\hat{L}^2}{2\Theta} + \hat{V}_{\mathrm{Ar-N_2}}(\{\mathbf{r}\}, \mathbf{R}_0, \vartheta, \varphi). \tag{2}$$

$\{\mathbf{r}\}$ and $\{\mathbf{p}\}$ are the positions and momenta of the classical (Ar) particles, $\mathbf{P}$ is the (translational) momentum

of the (N_2) molecule with particle coordinates at $\mathbf{R}_1$ and $\mathbf{R}_2$, $\hat{L}$ is its angular momentum operator, and Θ the momentum of inertia ($\hbar^2/2\Theta = 4.00345 \times 10^{-23}$ J). The coordinates ($\mathbf{R}_1$, $\mathbf{R}_2$) relative to the N_2 center of mass (at position $\mathbf{R}_0$) are given by the polar angles with the C_4 symmetry axes, ϑ and φ, $\mathbf{R}_{1,2} = \mathbf{R}_0 \pm (\sin\vartheta\cos\varphi, \sin\vartheta\sin\varphi, \cos\vartheta)\sigma^l_{\mathrm{N-N}}/2$. Since the N_2 vibrational mode has a high energy compared to the temperature we neglect the intramolecular potential and fix the distance $\sigma^l_{\mathrm{N-N}}$ between the N atoms. For model parameters for the L-J potentials $V_{\mathrm{Ar-Ar}}$, $V_{\mathrm{N-Ar}}$ between our particles, see Ref. [7].

The low-temperature anomalies mentioned in the introduction are usually attributed to the orientational degrees of freedom. In this spirit we assume that at low temperatures the time scales of the rotational degrees of freedom and the translational degrees of freedom separate and an adiabatic approximation is justified [9]. Now one can formally write down the partition function at temperature $T = \beta^{-1}/k_B$, where the translational momenta are integrated out.

$$Z(\beta) = \int d\{\mathbf{p}\}d\{\mathbf{P}\}\exp\{-\beta(T_{\mathrm{Ar}} + T^{(\mathrm{trans})}_{\mathrm{N_2}})\} \times \int d\{\mathbf{r}\}d\mathbf{R}_0 \exp\{-\beta V_{\mathrm{Ar-Ar}}\} \times \mathrm{tr}_{\vartheta,\varphi}[\exp\{-\beta\hat{\mathcal{H}}_{\mathrm{rot}}\}]. \quad (3)$$

The integration over the classical momentum space can be carried out immediately and we can define $W(\{\mathbf{r}\}, \mathbf{R}_0)$ as the unnormalized probability weight of the configuration $\{\{\mathbf{r}\}, \mathbf{R}_0\}$.

$$W(\{\mathbf{r}\}, \mathbf{R}_0) = \exp\{-\beta V_{\mathrm{Ar-Ar}}\}\mathrm{tr}_{\vartheta,\varphi}[\exp\{-\beta\hat{\mathcal{H}}_{\mathrm{rot}}\}]. \quad (4)$$

Thus, if we can work out the trace, we now can apply the Metropolis procedure and make a random walk through the phase space at a defined temperature.

For our system two limiting cases can be discussed immediately. If $\Theta = 0$ the ground state of the total problem will have cubic symmetry, since only $l = 0$ will give a contribution to the wave function ($l = 1$ would be very costly in energy). If $\Theta \to \infty$, we obtain the classical case and the lowest energy structure should have tetragonal symmetry.

Since we don't want to break the symmetry of our system (we know that at most the average has to have cubic symmetry) we separate our total Hamiltonian when expanding the trace in one cubic part $\hat{\mathcal{H}}_0$, which consists of the rotational kinetic energy and a cubic potential, obtained by symmetrization, and into a perturbance $\hat{\mathcal{H}}_1$, formed by the full potential minus the cubic potential, thus,

$$\hat{\mathcal{H}}_{\mathrm{rot}} = \hat{\mathcal{H}}_0 + \hat{\mathcal{H}}_1, \quad (5)$$

$$\hat{\mathcal{H}}_0 = \frac{\hat{L}^2}{2\Theta} + V(\{\mathbf{r}\}_{\mathrm{cub}}, \{\mathbf{R}\}), \quad (6)$$

$$\hat{\mathcal{H}}_1 = V(\{\mathbf{r}\}, \{\mathbf{R}\}) - V(\{\mathbf{r}\}_{\mathrm{cub}}, \{\mathbf{R}\}). \quad (7)$$

We restrict the dimensionality of the Hilbert space to the dimensionality four [9]. To have the best expansion in this symmetry class, we vary the four next neighbor shells within cubic symmetry and solve the eigenvalue problem.

$$\hat{\mathcal{H}}_0|\psi\rangle = \varepsilon_0|\psi\rangle. \quad (8)$$

Then we compute the Ar-Ar potential and choose the configuration $\{\mathbf{r}\}_{\mathrm{cub}}$ that minimizes the total energy $\varepsilon_0 + V_{\mathrm{Ar-Ar}}$.

In order to obtain thermal averages we use the Trotter product formula for the trace.

$$\mathrm{tr}_{\vartheta,\varphi}(\exp\{-\beta\hat{\mathcal{H}}_{\mathrm{rot}}\}) = \lim_{L\to\infty} \mathrm{tr}_{\vartheta,\varphi}[(\exp\{-\beta\hat{\mathcal{H}}_0/L\}\exp\{-\beta\hat{\mathcal{H}}_1/L\})^L], \quad (9)$$

where L denotes the Trotter dimension. The matrix elements in Eq. (9) are computed after linearization of the second factor with the wave functions from our minimalization procedure, see Sec. III. Since our present computations are done in low dimensional Hilbert spaces (with dimensions ≤ 4), these matrix elements were evaluated by numerical integration (over 60×60 points on the unit sphere), resulting in simple 4×4 matrices $\mathcal{A}$, and since $\mathcal{A}^L = (\cdots((\mathcal{A}^2)^2_1)^2_2\cdots)^2_{M-1}$ for $L = 2^M$, M integer, effectively only M matrix products have to be done to evaluate the trace. This allows us to work with giant values of L, see Sec. IV. We then use these numbers and apply standard techniques in a Monte Carlo simulation, see Ref. [9]. Results of these quantum Monte Carlo simulations are presented in Sec. IV.

III. THE GROUND STATE

In determining the wave function we restricted the variations until now on cubic variations of the four next neighbor shells of the rotator. Now we want the surrounding argon matrix to make a random walk through the phase space, but the new coordinates are only accepted if the total energy of the system is lowered. These calculations are carried out for *para*-N_2 and *ortho*-N_2.

We first sketch the way for obtaining the ground state for *para*-N_2, for details see Refs. [10–16] We put Ar particles with positions $\{\mathbf{r}_i\}$ on the fcc lattice sites $\{\mathbf{r}^0_i\}$, substitute a single Ar particle by a rigid rotator (N_2) with the center of mass located on the lattice site $\mathbf{R}_0$ and compute the symmetrized potential

$$\hat{V}^S(\{\mathbf{r}\}, \{\mathbf{R}\}, \vartheta, \varphi) = \sum_i [V_{\mathrm{N-Ar}}(R_1 - r_i) + V_{\mathrm{N-Ar}}(R_2 - r_i)]. \quad (10)$$

For fixed positions of the Ar particles we have to solve the eigenvalue problem with the Hamiltonian $\hat{\mathcal{H}}_{\mathrm{rot}}$ given by Eqs. (2), (5)–(7), and $\hat{\mathcal{H}}_1 = 0$ in this case.

Our potential $\hat{V}^S$ is of cubic symmetry, thus the Hamiltonian is invariant under operations with elements of the cubic group O_h. At low temperatures we are only interested in the lowest energy levels, in particular, of the ten possible eigenfunction symmetry types [14] only the solutions for the irreducible representations A_{1g} and T_{1u} of O_h. For *para*-N_2 we obtain the lowest energy eigenstate by utilizing A_{1g}. The energy eigenvalues $\varepsilon_k^{A_{1g}}$ (k is the angular momentum eigenvalue of the free rotator) are nondegenerate, the eigenfunctions are symmetric, $\varepsilon_0 = \varepsilon_0^{A_{1g}}$ denotes the ground state of the rotator. The eigenvalues $\varepsilon_k^{T_{1u}}$ are triply degenerate, an eigenfunction is antisymmetric and has a nodal line along one of the C_4 axes, $\varepsilon_1 = \varepsilon_1^{T_{1u}}$ denotes the lowest possible eigenvalue in this symmetry.

For the particular symmetry type ST we expand the eigenfunctions with symmetry adapted combinations of spherical harmonics [15] $X_{k,n}^{ST}$ (n distinguishes orthonormal functions for the same k and different coefficients for the magnetic numbers m);

$$\psi^{ST}(\vartheta,\varphi,\{\mathbf{r}_i\}) = \sum_{k,n} a_{k,n}^{ST}(\{\mathbf{r}_i\}) X_{k,n}^{ST}(\vartheta,\varphi). \qquad (11)$$

Energy eigenfunctions which minimize the energy should have minimal energy eigenvalues as functions of the $a_{k,n}^{ST}$'s, thus all first partial derivatives of the energy eigenvalues with respect to the a's are zero. Utilizing the Schrödinger equation and differentiation of the expectation value $\langle \psi^{ST}, \hat{\mathcal{H}}_0 \psi^{ST} \rangle = \varepsilon \sum_{k,n} (a_{k,n}^{ST})^2$ with respect to the $a_{k,n}^{ST}$ gives a numerical eigenvalue problem, where an eigenvector is given by an array of the a's for a particular eigenvalue ε. These numerical eigenvalues are the possible energy eigenvalues and the corresponding a's optimize the energy eigenfunctions (Ritz-Galerkin method) [16].

We then vary the positions of the neighbors (NN denoting nearest neighbors, 2N next nearest neighbors, nN the nth neighbors) in the volume V by a free variation of the coordinates up to the fourth neighbor shell and a variation of the density $\rho = N/V$, always accepting configurations with lower energy. For every coordinate combination we approximate the ground state wave function for the rotator with the Ritz-Galerkin method in the new potential of cubic symmetry. We finally obtain for the case of *para*-N_2 as the ground state a cubic lattice distortion with the zero pressure solid density $\rho\sigma^3_{\mathrm{Ar-Ar}} = 1.0669$, where all neighbor coordinates are changed in radial direction away from the rotator, $\mathbf{r}_i^{\mathrm{NN}} = \lambda^{\mathrm{NN}} \mathbf{r}_i^{0,\mathrm{NN}}$, $\mathbf{r}_i^{\mathrm{2N}} = \lambda^{\mathrm{2N}} \mathbf{r}_i^{0,\mathrm{2N}}$. We find a minimum in the total energy of the coupled system for $\lambda^{\mathrm{NN}} = 1.0128$, $\lambda^{\mathrm{2N}} = 0.9997$, $\lambda^{\mathrm{3N}} = 1.0016$, and $\lambda^{\mathrm{4N}} = 1.0018$, where the change of the volume spanned by the first neighbors is very close to the change of the volume spanned by the fourth neighbors, see Fig. 1(a). The wave function for the *para*-N_2 equilibrium ground state with energy ε_0 (the ground state energy difference between the *para*-N_2 dilution and the pure Ar case is 350 K) has six maxima representing the enhanced probability for the rotator orientation in one of the (100) directions. The resulting wave function for the

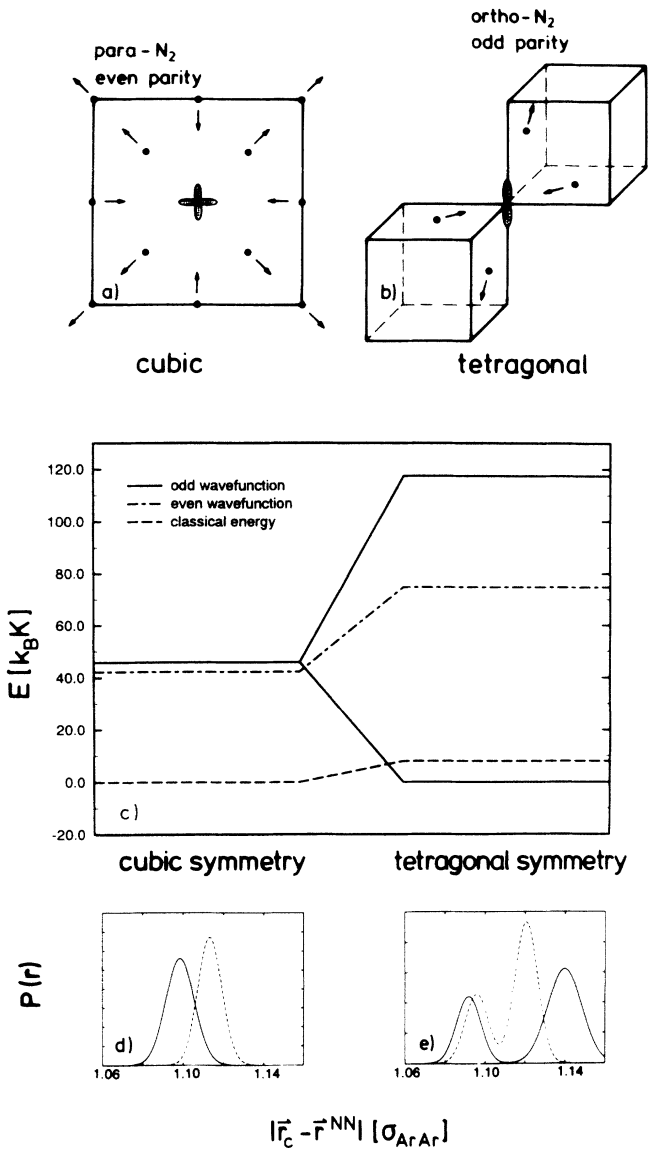

FIG. 1. Ground state symmetry [(a) and (b)], energy levels (c) for *para*-N_2 and *ortho*-N_2, and next neighbor distribution functions [(d) and (e)] at finite temperatures; the left column shows results for *para*-N_2, the right column for *ortho*-N_2. (a) Ground state lattice deformation near the rotator impurity for *para*-N_2, the points are centers of classical (Ar) particles, the central particle is the rotator impurity (N_2). (b) Ground state lattice deformation near the rotator impurity for *para*-N_2, symbols are the same as (a). (c) Rotator energy levels. Left side: cubic symmetry of Ar atoms, so that the total energy for *para*-N_2 is minimized; the first excited state (odd wave function) is triply degenerate. Right side: tetragonal symmetry of Ar atoms, so that the total energy is minimized with odd wave functions; the upper state is now twofold degenerate. The classical Ar-Ar energy of the environment in cubic and tetragonal symmetry is shown for comparison. (d) Nearest-neighbor distribution functions $P(\{\mathbf{r}^{\mathrm{NN}}\})$ in the directions $\Pi\,(\pm1,\pm1,0)$ (in arbitrary units) around the impurity (at position $\mathbf{r}_C = \mathbf{R}_{1,2}$) at finite temperatures for the pure (Ar) system (full line) and *para*-N_2 (dashed line). (e) Same as (d), but for classical N_2 (full line) and *ortho*-N_2 (dashed line).

next energy level, ε_1, is energetically triply degenerate, because of the cubic symmetry, the energy difference is $\varepsilon_1 - \varepsilon_0 = 3.6$ K, see Fig. 1(c).

These wave functions can now be utilized for the evaluation of the trace in Eq. (9) and thus for a quantum Monte Carlo (MC) calculation at nonzero temperatures [9], see Sec. IV.

In case of *ortho*-N_2 we can no longer find the ground state in terms of even wave functions and thus utilize the wave functions of the symmetry class T_{1u} for finding the ground state of the system again by free variation of the neighbor coordinates and utilizing Eq. (9) in the limit $\beta \to \infty$ with the four lowest energy states obtained in the ground state configuration for *para*-N_2. We finally find a *tetragonal* ground state lattice deformation in this case, see Fig. 1(b). The energy levels are not any longer triply degenerate, but split into one oriented ground state with lowest energy [see Fig. 1(c)] and a double degenerate excited state (the energy difference is 117.5 K) with mutual perpendicular orientation to each other and to the ground state. The rotational energy of the oriented ground state for *ortho*-N_2 is even lower than the ground state energy in case of the nonoriented case (*para*-N_2), the energy difference is 42.2 K, see Fig. 1(c). The ground state energy difference for the total system between the tetragonal and the cubic symmetry (including the classical Ar-Ar interaction energy, which increases by 8 K), is 34.2 K, see Fig. 1(c).

IV. QMC RESULTS AT FINITE TEMPERATURES

At finite temperatures the trace is taken with symmetric wave functions from Sec. II for *para*-N_2 and with antisymmetric wave functions for *ortho*-N_2. Thermal averages $\langle\ \rangle$ are taken with a MC procedure [17–19] according to the measure in $Z(\beta)$, utilizing the Trotter decomposition [9,17], Eq. (9).

We are interested in low-temperature phenomena and assume that the thermal properties at very low temperatures are predominantly determined by the lowest energy states. In the cubic symmetry class A_{1g} the two lowest rotator states have an energy difference of $20\hbar^2/2\Theta \approx 57$ K, for zero external potential, the energy difference between the two lowest states for the annealed rotator ($A_{1g} - T_{1u}$) is $2\hbar^2/2\Theta \approx 6$ K, reducing to 3 K in the relaxed Ar surrounding (see Sec. III). The rotator states in the relaxed cubic Ar environment (see Sec. III) are obtained by a variational method employing states with $l \leq 12$; convergence was obtained already for $l \geq 6$ [10]. We checked the quality of our "low level" approximation by a comparison of low-temperature specific heat data for the annealed rotator in a fixed Ar surrounding of cubic symmetry and wave functions obtained with the methods of Sec. III with specific heat data obtained via the Trotter-Suzuki formula [17] and free rotator eigenstates up to $l = 14$ [20]. The data obtained in these two ways agree precisely for temperatures below 1 K, see Table I, and still are roughly in mutual agreement for $T < 10$ K. The classical high-temperature limit cannot be reached within our current restriction to a low-dimensional Hilbert space, of course. The error in thermal averages of observables resulting from the application of the Trotter decomposition with Trotter index L is proportional to inverse powers of L [21]. The convergence of our results with respect to L was checked with Trotter-scaling plots of all quantities investigated for a fairly large set of temperatures, including the lowest and highest one. As the end of Sec. II notes, the low dimension of our Hilbert space allows us to work with arbitrarily large Trotter dimensions L, and thus the error associated with the finiteness of L can be made extremely small. For the thermal averages over identical paths in the phase space of the classical degrees of freedom we find a plateau in the scaling plots for 2^{20} K $< LT < 2^{30}$ K with a relative error less than 10^{-6}, for larger L T rounding effects set in.

TABLE I. Specific heat c_V [k_B] of the annealed rotator in a static cubic lattice versus temperature. Column a: results with free rotator eigenstates ($l \leq 2$) [20]; column b: results with free rotator eigenstates ($l \leq 5$) [20]; column c: results with free rotator eigenstates ($l \leq 14$) [20]; column d: results with four symmetry adapted wave functions (see Secs. III and IV). The number in brackets denotes a multiplicative power of ten.

	Specific heat			
T [K]	a	b	c	d
0.25	1.5[-6]	0.0012	0.0003	0.0003
0.50	0.0040	0.1351	0.1075	0.1076
1.00	0.3078	0.9662	1.0014	0.8940
2.00	1.0231	0.9297	1.0291	0.7318
4.00	0.5036	0.4205	0.3295	0.2064

The specific heat of our total system is presented in Fig. 2. At low temperatures we obtain the classical value, since the N_2 contribution to the energy fluctuation is small in the system $(N_2)_x(Ar)_{1-x}$ in the dilute limit, $x \to 0$. Since our Monte Carlo treatment of positions is classical, these results cannot be compared to experi-

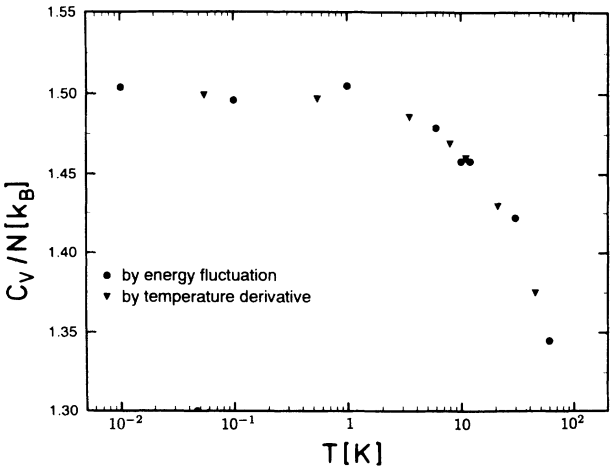

FIG. 2. Specific heat C_V versus temperature of the system $(N_2)_x$ $(Ar)_{1-x}$ for $x = 0.002$. Monte Carlo results (triangles: C_V obtained by a temperature derivative of energy simulation data; circles: C_V obtained from energy fluctuations).

ments, of course: rather Fig. 2 is important as a check that thermal equilibrium in the simulation is achieved down to the lowest temperatures.

At finite temperature the width of the real space correlation function is of special interest, since this property is principally available by measuring the Debye Waller factor $\exp(-2W)$ with,

$$2W = \langle(\mathbf{qu})^2\rangle, \tag{12}$$

where $\mathbf{q}$ denotes the change of momentum of an elastically scattered particle and $\mathbf{u}$ is the displacement vector. In a classical treatment of sound one generally finds the following proportionality in a harmonic approximation [22]:

$$2W \propto (k_B T)C, \tag{13}$$

where C denotes the relevant elastic modulus. Since we are working with only one impurity, we choose the displacement vector,

$$\mathbf{u} = \delta(\mathbf{R}_{N_2} - \mathbf{r}_{Ar}^{NN}), \tag{14}$$

and for $\mathbf{q}$ a permutation Π of $(\pm1, \pm1, 0)$

$$\mathbf{q} = \Pi\ (\pm1, \pm1, 0). \tag{15}$$

At low temperatures $(\mathbf{qu})^2 = q^2u^2$, thus, if the harmonic approximation is valid, u^2/T should be a constant. We perform our simulations with four different central impurity particles: *ortho*-N_2, *para*-N_2, *classical*-N_2 and Ar. In the case, that Ar is the "impurity", $\exp(-2W)$ is the Debye Waller factor, in the three other cases $\exp(-2W)$ has the signification of a *pseudo*-Debye Waller factor. For *ortho*-N_2 and *classical*-N_2, we obtain a double peak distribution, where the relative weight of the peaks are 1:2, due to the tetragonal distortion of the fcc lattice, see Figs. 1(d), and 1(e). We compute at different temperatures the radial distribution function and fit the results obtained for *para*-N_2 and Ar with a simple Gaussian, in other cases with double Gaussians, respecting the relative weight of 1:2 of the peaks. In Figs. 3 and 4 the widths of the Gaussians are plotted versus temperature. In Fig. 3 the pure Ar system shows classical, harmonic behavior at temperatures below 10 K (remember that the translational degrees of freedom are treated classically and the computations are carried out at constant density). At higher temperatures the atoms move more in the repulsive part of their potential and u^2/T decreases, see Table II. In the case of *ortho*-N_2 [see Fig. 4] the behavior is quite similar to the pure Ar case, but due to the larger volume of the N_2 molecule the peak position for the nearest neighbor Ar is shifted to larger distances from the molecule and the width of the distribution is smaller, thus, the system has a higher elastic module. If *classical*-N_2 is the impurity [Fig. 3], every peak shows qualitatively the same behavior as the pure Ar system, but the widths of the two peaks are different. This shows, that the effective "spring constants" of the central particle to the next neighbor are dependent of the direction, namely, whether the next neighbor is sitting in the plane perpendicular to the orientation or not. The differences in the width of the two different peaks of the radial distribution function indicates, that the local, static deformation due to the presence of the N_2 rotator is anharmonic. Nevertheless the widths of the peaks obey scaling laws with temperatures obtained generally by doing the harmonic approximation. Similar to the classical case, *ortho*-N_2 [Fig. 4] causes an anharmonic,

TABLE II. The temperature dependence of the averaged distance between the nearest-neighbor particle and the rotator (*para*-N_2), $\langle r^{NN}\rangle$, in the directions $\Pi(\pm1, \pm1, 0)$, and the ratio of the averaged squared displacement vector and the temperature, $\langle u^2\rangle/T$, see Eq.(14).

T [K]	$\langle r^{NN}\rangle$ (σ_{Ar-Ar})	$\langle u^2\rangle/T$ $(10^{-5}\ \sigma^2_{Ar-Ar}/K)$
10	1.1136	5.87
1	1.1142	6.89
0.1	1.1134	6.66
0.01	1.1134	7.04

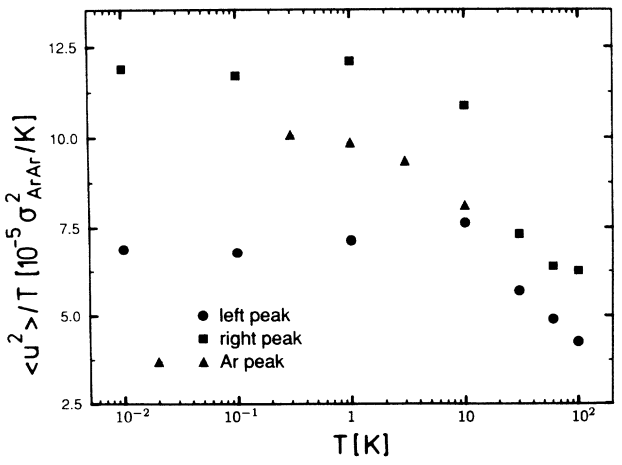

FIG. 3. Normalized widths $\langle u^2\rangle/T$ versus temperature of the nearest-neighbor distribution function [see Figs. 1(d) and 1(e)] for classical N_2 (squares: large distance peak; circles: small distance peak) and Ar (triangles: line for visual help).

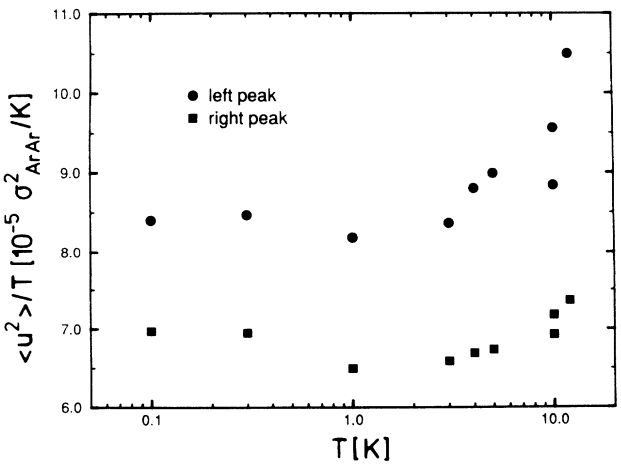

FIG. 4. Normalized widths $\langle u^2\rangle/T$ versus temperature of the nearest neighbor distribution function [see Fig. 1(e)] for *ortho*-N_2 (circles: small distance peak; squares: large distance peak).

static deformation, and at low temperatures up to 10 K classical harmonic approximation turns out to be valid. With increasing temperatures, not only the ground state is occupied and, thus, the rotational fluctuations cause translational fluctuation of the next neighbors. With a higher dimensional Hilbert space, we assume this effect to set in already at lower temperatures, thus, in the whole range of temperature the quantum-mechanical rotator allows the surrounding to fluctuate more than the classical rotator.

It is of great physical interest to consider also the dynamical behavior of the rotator impurity in its Ar environment. Since Monte Carlo dynamics is not directly linked to the dynamics in real time, in principle one should then treat the (classical) dynamics of the Ar atoms by molecular dynamics methods, but this is out of the scope here and will be considered in future work. But a qualitative insight into the rotational diffusion of the rotator can already be gained in terms of the stochastic dynamics provided by the Monte Carlo process. This is because for a rotational diffusion that is much slower than the typical phonon times the phonons act like a heat bath inducing random reorientations of the rotator, and a master equation description as realized by the Monte Carlo process is not unreasonable (see also Ref. [18]). Of course, there is still an unknown conversion factor from the Monte Carlo "time" to the physical time, which could only be fixed by a more realistic treatment.

The orientational correlation function $\psi(t)$ for classical rotators often used in the literature [23,24] is

$$\psi(t) = \langle \mathbf{n}(t)\mathbf{n}(0) \rangle \quad , \tag{16}$$

where $\mathbf{n}(t)$ is the normalized vector indicating the orientation of the molecule at time t. In Ref. [23] the following time dependency of the correlation function is derived analytically for a classical rotator coupled to a stochastic torque:

$$\psi(t) = \exp\{-A(t/\tau + \exp[-t/\tau] - 1)\} \quad , \tag{17}$$

where τ is a relaxation time and A an adjustable constant of order one. Also a numerical study [24] within the Langevin model of a classical rotator showed an exponential (and faster) decay of the correlation function with time.

Due to the indistinguishability of the nitrogen nuclei the straightforward generalization of Eq. (16) to the quantum case results in zero values in all $\mathrm{tr}_{\vartheta,\varphi}\{\mathbf{n}(t)\}$. Thus, we define an appropriate time correlation function $\Phi(t)$ with properties $\Phi(0) = 1$ and $\lim_{t\to\infty} \Phi(t) = 0$:

$$\Phi(t) = \frac{\langle \mathrm{tr}_{\vartheta,\varphi}\{\hat{z}^2\} - \mathrm{tr}_{\vartheta,\varphi}\{\hat{r}^2/3\}\rangle_C(t)}{\langle \mathrm{tr}_{\vartheta,\varphi}\{\hat{z}^2\} - \mathrm{tr}_{\vartheta,\varphi}\{\hat{r}^2/3\}\rangle_C(t=0)}, \tag{18}$$

with the operator $\hat{z}$ projecting on the (001) direction. $\langle\rangle_C$ (t) denotes the statistical average over configurations at time t (t is taken in Monte Carlo steps). Since we are working in the adiabatic approximation, we measure the orientation of the surrounding Ar matrix and not the quantum dynamics. In particular, Eq. (18) enables us to clarify whether the relaxation of the deformed Ar surrounding is guaranteed within realistic MC times. Only if the length of the MC runs is large enough that a significant decay of $\Phi(t)$ has occurred are the MC data sufficiently decorrelated to allow statistically significant estimates. Thus, a study of $\Phi(t)$ is also mandatory to establish the actual accuracy. In Fig. 5 we present a plot of some typical relaxation functions. Surprisingly our results can be described by a stretched exponential,

$$\Phi(t) \propto \exp\{-(t/\tau)^\gamma\} \quad . \tag{19}$$

The exponent γ has values near one at very low temperatures and seems to decrease with increasing temperature, see Table III. For the data obtained in this paper we work with a statistical effort of 20 000 Monte Carlo steps, the system consists of 500 particles. Even with this effort, for quantities like γ it is still very difficult to

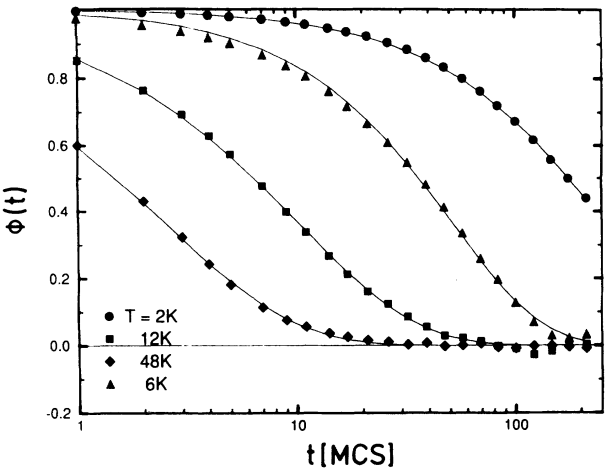

FIG. 5. Orientational correlation function $\Phi(t)$ of *ortho*-N_2 versus Monte Carlo steps for different temperatures [circles: $T = 2$ K; triangles: $T = 6$ K; squares: $T = 12$ K; and diamonds: $T = 48$ K, lines are fits through the data with Eq.(19)].

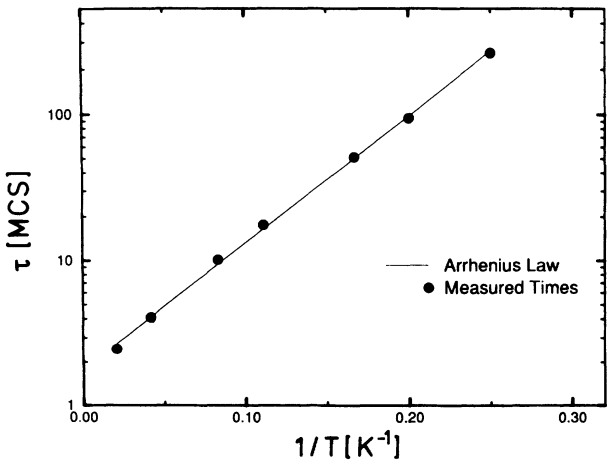

FIG. 6. Arrhenius plot of the relaxation time τ (circles: τ obtained from fits through simulation data of Fig. 5; line: Arrhenius law interpolation line).

TABLE III. Exponent γ in the stretched exponential form for the rotator time correlation function $\Phi(t) \propto \exp[-(t/\tau)^{\gamma}]$.

T [K]	τ [MCS]	γ
4	260	0.99
6	51	1.00
12	10	0.81
48	2.5	0.72

judge if this exponent is temperature dependent or not due to statistical noise and long relaxation times.

If we make an Arrhenius plot of the orientation relaxation time τ, see Fig. 6, we obtain an apparent activation energy of 20 k_B T, which is much lower than the local barrier for turning a classical N_2 molecule from one preferred orientation to another. This would cost about 70 k_BT.

V. SUMMARY AND OUTLOOK

We presented the results of classical and quantum Monte Carlo simulations of a rotator impurity N_2 in Ar. For *para*-N_2 we obtain a symmetric lattice deformation with harmonic excitations at finite temperatures. For *ortho*-N_2 we obtain an asymmetric lattice deformation in the tetragonal structure, the lattice vibrations are nevertheless harmonic at low temperatures. The orientational degree of freedom relaxes according to an Arrhenius law.

In a future work we are going to include the interactions of many quantum rotators in order to get a better understanding of the quantum phenomena in orientational glasses at low temperatures. In that case we treat the translational degrees of freedom of the Ar particles quantum mechanically by path integral Monte Carlo techniques [17] and the rotators with a low-temperature expansion in higher Hilbert space dimensions.

ACKNOWLEDGMENTS

This research was carried out in the framework of the Sonderforschungsbereich 262 der Deutschen Forschungsgemeinschaft. P.N. thanks the DFG for financial support (Heisenberg foundation). The computations were carried out on the Cray YMP computer of the HLRZ at Jülich.

[1] A. Loidl, Ann. Rev. Phys. Chem. **40**, 29 (1989); U.T. Höchli, K. Knorr, and A. Loidl, Adv. Phys. **39**, 405 (1990); K. Binder and J.D. Reger, *ibid.* **41**, 547 (1992).

[2] K. Knorr and A. Loidl, Phys. Rev. Lett. **57**, 460 (1986).

[3] K.H. Michel, Phys. Rev. B **35**, 1405 (1987); **35**, 1414 (1987).

[4] H.-O. Carmesin and K. Binder, Europhys. Lett. **4**, 269 (1987); J. Phys. A **21**, 4053 (1988); D. Hammes, H.-O. Carmesin, and K. Binder, Z. Phys. B **76**, 115 (1989).

[5] *Amorphous Solids, Low Temperature Properties*, edited by W.A. Phillips (Springer, Berlin, 1980).

[6] V.I. Gol'danskiij, L.I. Trakhtenberg, and V.N. Fleurov, *Tunneling Phenomena in Chemical Physics* (Gordon and Breach, New York, 1981); W. Press, *Single-Particle Rotations in Molecular Crystals*, Springer Tracts in Modern Physics Vol. 92 (Springer, New York, 1981); A. Hüller, Z. Phys. B **36**, 215 (1980); A. Hüller and L. Baetz, *ibid.* **72**, 47 (1988); A. Würger, *ibid.* **76**, 65 (1989); K. Parlinski and H. Grimm, Phys. Rev. B **37**, 1925 (1988).

[7] H.-O. Carmesin, Ph.D. thesis, University of Mainz, 1988 (unpublished). Lennard-Jones potential parameters are $\sigma_{Ar-Ar} = 3.4$ Å, $\sigma_{N-N} = 3.31$ Å, $\sigma_{N-Ar} = 3.35$ Å, $\varepsilon_{Ar-Ar} = 1.67 \times 10^{-21}$ J, $\varepsilon_{N-Ar} = 0.927 \times 10^{-21}$ J, $\varepsilon_{N-N} = 0.515 \times 10^{-21}$ J. The distance between the N atoms is $\sigma^{l}_{N-N} = 2 \times 0.1646 \times 3.31$ Å.

[8] H. Klee, H.-O. Carmesin, and K. Knorr, Phys. Rev. Lett. **61**, 1855 (1988).

[9] W. Helbing, P. Nielaba, and K. Binder, Phys. Rev. B **44**, 4200 (1991); the results obtained in this paper are hampered by detailed balance failures and results for the energies and the neighbor structures should be replaced by the recent results, where appropriate.

[10] P. Nielaba and K. Binder, Europhys. Lett. **13**, 327 (1990).

[11] A.F. Devonshire, Proc. R. Soc. London, Ser. A **153**, 601 (1936).

[12] P. Sauer, Z. Phys. **194**, 360 (1966).

[13] H.U. Beyeler, Phys. Status Solidi B **52**, 419 (1972).

[14] M. Tinkham, *Group Theory and Quantum Mechanics* (McGraw-Hill, New York, 1964).

[15] S.L. Altmann and A.P. Cracknell, Rev. Mod. Phys. **37**, 19 (1965).

[16] See S.G. Michlin, *Variationsmethoden der Mathematischen Physik* (Akademie, Berlin, 1962).

[17] *Quantum Monte Carlo Methods*, edited by M. Suzuki, Springer Series in Solid State Sciences Vol. 74 (Springer, New York, 1987); B.J. Berne and D. Thirumalai, Annu. Rev. Phys. Chem. **37**, 401 (1986); *Quantum Simulations of Condensed Matter Phenomena*, edited by J.D. Doll and J.E. Gubernatis (World Scientific, Singapore, 1990); *Monte Carlo Methods in Statistical Physics*, edited by K. Binder, Topics in Current Physics Vol. 7 (Springer, Berlin, 1986).

[18] K. Binder and D.W. Heermann, *Monte Carlo Simulation in Statistical Physics*, Springer Series in Solid State Sciences Vol. 80 (Springer, Berlin, 1988).

[19] The Monte Carlo simulation was done with N=500 particles at constant density $\rho\sigma^3_{Ar-Ar} = 1.0669$, a typical run with 20 000 Monte Carlo steps took about 6 CPU hours on a Cray YMP computer.

[20] Convergence of the quantum Monte Carlo results to the quantum limit utilizing the Trotter-Suzuki formula [17] was obtained with a Trotter index $L > 1000$ for $l \leq 5$ and $L > 2000$ for $l \leq 14$.

[21] R.M. Fye, Phys. Rev. B **33**, 6271 (1986); J. Stat. Phys. **43**, 827 (1986); R.M. Fye and R.T. Scalettar, Phys. Rev. B **36**, 3833 (1987).

[22] N.W. Ashcroft and N.D. Mermin, *Solid State Physics* (Holt, Rinehart and Winston, New York, 1976).

[23] W.A. Steele, J. Chem. Phys. **38**, 2404 (1963); **38**, 2411 (1963).

[24] R. Gerling and A. Hüller, Z. Phys. B **40**, 209 (1980).